Journal of Biomechanics 120 (2021) 110362

Contents lists available at ScienceDirect

Journal of Biomechanics

journal homepage: www.elsevier.com/locate/jbiomech
www.JBiomech.com

Optical motion capture accuracy is task-dependent in assessing wrist motion

Brian McHugh [a], Bardiya Akhbari [a], Amy M. Morton [b], Douglas C. Moore [b], Joseph J. Crisco [a,b,*]

[a] Center for Biomedical Engineering and School of Engineering, Brown University, Providence, RI 02912, United States
[b] Department of Orthopedics, The Warren Alpert Medical School of Brown University and Rhode Island Hospital, Providence, RI 02903, United States

ARTICLE INFO

Article history:
Accepted 22 February 2021

Keywords:
Optical motion capture
Wrist
Kinematics
Soft tissue artifact
Accuracy

ABSTRACT

Optical motion capture (OMC) systems are commonly used to capture *in-vivo* three-dimensional joint kinematics. However, the skin-based markers may not reflect the underlying bone movement, a source of error known as soft tissue artifact (STA). This study examined STA during wrist motion by evaluating the agreement between OMC and biplanar videoradiography (BVR). Nine subjects completed 7 different wrist motion tasks: doorknob rotation to capture supination and pronation, radial-ulnar deviation, flexion–extension, circumduction, hammering, and pitcher pouring. BVR and OMC captured the motion simultaneously. Wrist kinematics were quantified using helical motion parameters of rotation and translation, and Bland-Altman analysis quantified the mean difference (bias) and 95% limit of agreement (LOA). The rotational bias of doorknob pronation, a median bias of −4.9°, was significantly larger than the flexion–extension (0.7°, $p < 0.05$) and radial-ulnar deviation (1.8°, $p < 0.01$) tasks. The rotational LOA range was significantly smaller in the flexion–extension task (5.9°) compared to pitcher (11.6°, $p < 0.05$) and doorknob pronation (17.9°, $p < 0.05$) tasks. The translation bias did not differ between tasks. The translation LOA range was significantly larger in circumduction (9.8°) compared to the radial-ulnar deviation (6.3°, $p < 0.05$) and pitcher (3.4°, $p < 0.05$) tasks. While OMC technology has a wide-range of successful applications, we demonstrated it has relatively poor agreement with BVR in tracking wrist motion, and that the agreement depends on the nature and direction of wrist motion.

1. Introduction

Accurately quantifying three-dimensional (3D) joint kinematics during *in-vivo* wrist motion is essential for a detailed understating of joint function, investigating pathologies and assessing the success of therapies (Aizawa et al., 2010). The wrist has two primary degrees-of-freedom (DOF), defined by the anatomical directions of flexion–extension and radial-ulnar deviation. Most activities of daily living are accomplished with combinations of these primary motions, such as circumduction and dart thrower's motion (Garg et al., 2014). Circumduction describes a circular motion of the hand. Dart thrower's motion describes wrist movement along an oblique plane from radial-extension to ulnar-flexion. Dart thrower's motion is observed in many functional tasks, such as hammering (Wolfe et al., 2006). Because the wrist mainly executes coupled motions, it is important to study the accuracy of measurement systems in coupled motions and in all of its 6-DOF.

Optical motion capture (OMC) is commonly used to quantify *in-vivo* joint kinematics (Miranda et al., 2013; Schmidt et al., 1999; Small et al., 1996). OMC systems provide a non-invasive method to capture 3D joint kinematics using markers that adhere to the skin. OMC is advantageous for large capture volumes that study multiple joints (Miranda et al., 2013). However, skin-based markers are limited by the error in mapping the skin maker data to the underlying bone movement. This error is referred to as soft tissue artifact (STA) (Cutti et al., 2005; Miranda et al., 2013). Skin movement and marker placement differs for different joints, making STA joint specific. STA has been assessed using biplanar videoradiography (BVR) (Brainerd et al., 2010; Miranda et al., 2011; Tashman and Anderst, 2003) as the gold standard in the ankle (Kessler et al., 2019), knee joint (Miranda et al., 2013), and hip (D'Isidoro et al., 2020).

Our study aims to evaluate the accuracy of OMC in measuring *in-vivo* wrist motions across various dynamic uni-directional and

* Corresponding author at: Bioengineering Laboratory, Department of Orthopedics, The Warren Alpert Medical School of Brown University and Rhode Island Hospital, 1 Hoppin Street, CORO West, Suite 404, Providence, RI 02903, United States.

E-mail addresses: brian_mchugh@alumni.brown.edu (B. McHugh), bardiya_akhbari@brown.edu (B. Akhbari), amy_morton1@brown.edu (A.M. Morton), douglas_moore@brown.edu (D.C. Moore), joseph_crisco@brown.edu (J.J. Crisco).

https://doi.org/10.1016/j.jbiomech.2021.110362
0021-9290/

coupled tasks using BVR as the gold standard. Previous studies have established the submillimeter and sub degree accuracy of BVR in tracking wrist and total wrist arthroplasty motion (Akhbari et al., 2019c, 2019b).

2. Methods

Subjects: Nine subjects (age: 56.9 ± 5.5y, females: 8, right-side: 8) were recruited after institutional review board approval. Prior to data collection, all subjects were pre-screened with hand and wrist X-rays to rule out any bony pathology. A computed-tomography (CT) scan (80kVp and 80 mA) of the hand, wrist, and forearm was acquired ($0.39 \times 0.39 \times 0.625$ mm^3) and imported into Mimics v19 (Materialise, Ann Arbor, MI). The radius and third metacarpal (MC3) were segmented semi-automatically for further use in BVR tracking (Akhbari et al., 2019c).

Data Collection: BVR and OMC data were collected (200 Hz for both systems, TTL pulse synchronized) in the W.M. Keck Foundation XROMM facility at Brown University (Providence, RI) (Miranda et al., 2011). The BVR system used in this experiment was previously validated and documented in detail (Akhbari et al., 2019c; Miranda et al., 2011). X-ray beams were produced at exposure parameters of 60 kV and 80 mA. A calibration cube was used to calibrate the X-ray systems, and the videoradiographs were dedistorted with a distortion grid in XMALab (http://www.xromm.org/xmalab/) (Knörlein et al., 2016).

Eight OMC cameras (Oqus 5-series, Qualisys, Gothenburg, Sweden) were placed around the XROMM system along a circular perimeter. Individual retroreflective spheres were placed on the dorsal surface of the forearm over the radius (n = 4, 6.4 mm dia.) and the dorsal side of the hand over the MC3 (n = 4, 6.4 mm dia.) using double-sided adhesive (Fig. 1). A cross-calibration cylinder was captured by both systems simultaneously to generate a transformation matrix to directly compare the two systems (Knörlein et al., 2016).

Experimental Procedure: Subjects performed 7 dynamic tasks: 4 unidirectional anatomical movements and 3 coupled movements (Fig. 2). Subjects were coached on how to complete the task prior to capturing the motion, and a metronome (90 bpm) was used to assist in maintaining a constant speed. For all tasks, subjects were instructed to limit the movement of their elbow and shoulder.

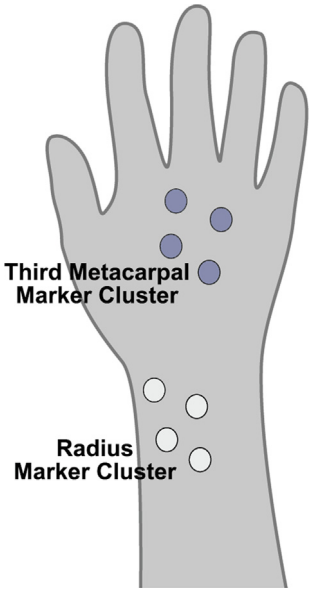

Fig. 1. Marker Placement. A cluster (n = 4, 6.4 mm dia.) of retroreflective markers placed on the dorsal side of the third metacarpal (MC3) and a cluster (n = 4, 6.4 mm dia.) of retroreflective markers placed on the dorsal side of the radius was used for optical motion capture (OMC) data collection.

Task Description: Flexion-extension and radial-ulnar deviation were performed while the subjects were coached to focus on the isolated plane of motion. A fixture with a plastic T-shaped handle attached to one side of a doorknob mechanism (DK) was used to capture forearm pronation (DKPro) and forearm supination (DKSup).

The three coupled motion tasks performed were hammering (hammer), a pouring motion with a pitcher (pitcher), and circumduction (Fig. 2). Subjects were provided a hammer to repeatedly emulate a hammering motion from radial-extension to ulnar-flexion. For the pouring task, subjects mimicked a "teacup" pour with a weighted pitcher (1 kg) and held the pouring pose. For the circumduction task, subjects were instructed to move their wrist about a path that traced a circle.

Anatomical Coordinate System: An anatomical coordinate system was created from anatomical landmarks on the radius (RCS) and MC3 (MCS) as previously described (Fig. 3) (Akhbari et al., 2020, 2019a).

Data Processing: To compute wrist kinematics from the BVR data, a partially segmented CT volume of each bone, and videoradiographs from both X-ray sources, were imported into an open-source 2D-to-3D image registration software, Autoscoper (https://simtk.org/projects/autoscoper) (Akhbari et al., 2019c). An auto-registration algorithm was used to compute Digital Reconstructed Radiograph (DRR) projections from each partial CT bone volume and optimize alignment with the two BVR videoradiograph views. An initial manual position of the radius DRR was aligned with the radiographs by the user. For MC3 tracking, the combined second metacarpal bone (MC2) and MC3 positions were used to reduce the overlap causing alignment errors (Akhbari et al., 2019c). The output of the MC2 and MC3 position was transformed to initialize the MC3. An auto-registration algorithm optimized the initial position of the radius and MC3 in each BVR frame.

The OMC kinematic data was generated using Visual3D (C-Motion Inc., Germantown, MD). Utilizing the transformation matrix from the cross-calibration cylinder, the MCS and RCS from BVR were transformed into the OMC space. The MCS and RCS were loaded into Visual3D to construct an anatomically based coordinate system identical to the coordinate system used in BVR kinematic calculations. A transformation matrix for the radius marker cluster and the MC3 marker cluster was constructed containing the rotation and translation component at each frame.

Kinematic Analysis: Kinematic analysis was performed in MATLAB (R2018a, The MathWorks Inc., Natick, MA). For each subject, all tasks were analyzed to find the frame closest to the neutral position, which was defined as the minimum difference between the MCS and RCS. OMC and BVR-calculated motions were reported as the MC3 position with respect to the radius and relative to the neutral position. Helical axes of motion parameters were used to describe the kinematics (Crisco et al., 2005a; Panjabi et al., 1981). The rotation about the screw axis (ϕ) described total rotation of the wrist. Wrist translation was defined by the total translation along the screw axis.

Data and Statistical Analysis: The data for non-cyclic tasks (pitcher, DKSup and DKPro) was cropped to remove static positions. The start of the motion was determined when the derivative of the motion (degrees vs. frames) was greater than 0.04°/frames and the end of the motion was defined when the derivative was less than 0.04°/frames for the remainder of the task, after finding the starting position.

Bland-Altman analysis was used to quantify the agreement between OMC and the gold standard BVR. Bias was reported using

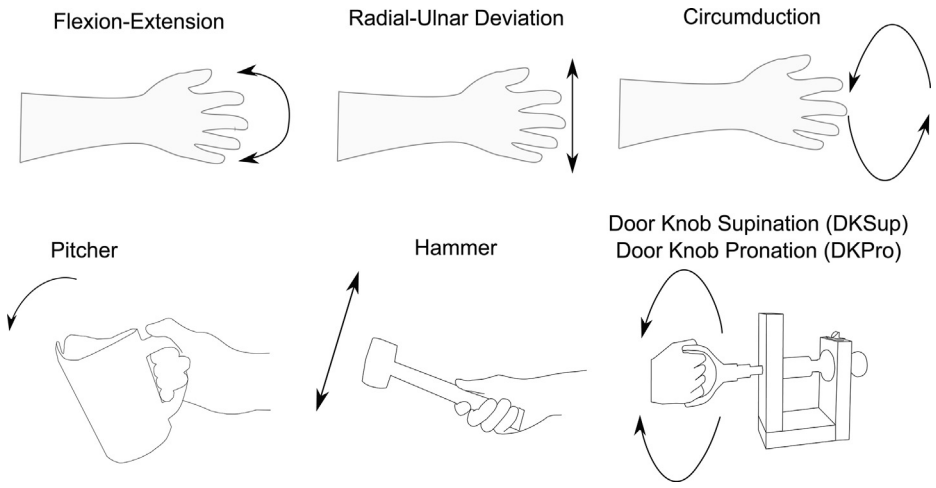

Fig. 2. Tasks. All subjects performed seven motion tasks (doorknob rotations were captured separately) as part of the experimental procedure.

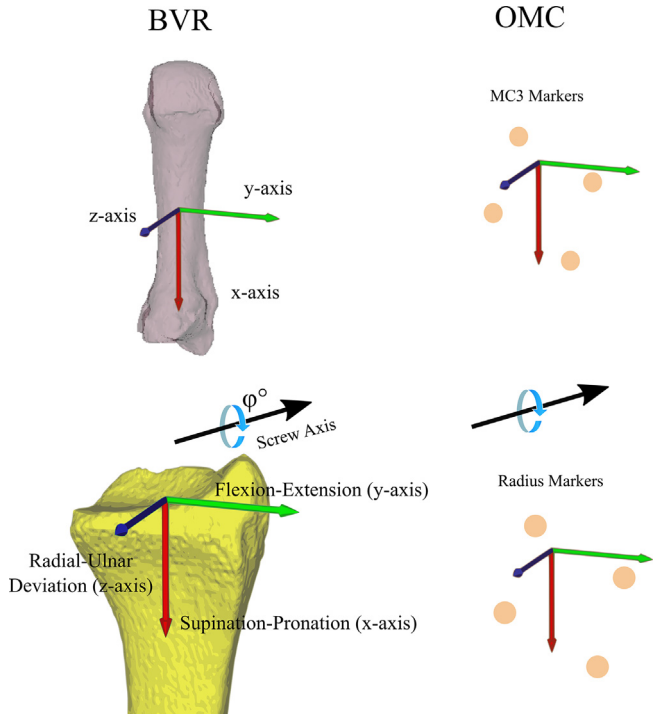

Fig. 3. Coordinate System Definition. The radius anatomical coordinate system (RCS) and third metacarpal (MC3) coordinate system (MCS) were constructed from anatomical landmarks during biplanar videoradiography (BVR) data processing. A transformation matrix describing the position of the markers as a rigid body represented the coordinate system of the markers (OMC). The rotation about the x-axis represents supination (−) pronation (+) plane, the rotation about the y-axis represents the flexion (+) extension (−) plane, and the rotation about the z-axis represents the radial (−) ulnar (+) plane.

the mean difference (MD) of BVR and OMC (BVR – OMC), the variation about the MD was reported using 95% limits of agreement (LOA) (MD ± 1.96*SD), that is, the interval within which 95% of differences between BVR and OMC are expected to lie (Bland and Altman, 1986). A Friedman test ($p < 0.05$) and post-hoc multiple comparisons (PRISM 8.0, GraphPad Software, La Jolla, CA) was used to test for significant differences in the bias and LOA range (difference between upper and lower LOA) between tasks.

A linear regression analysis was performed to determine if bias was associated with measurement size. The slopes of the linear regressions of all subjects for each task were compared to a hypothetical mean of 0.00 (i.e., bias did not differ with measurement size) via a one-sample *t*-test.

3. Results

The bias for ϕ varied across tasks with median values ranging from −4.9° to 1.8°, with the largest magnitudes of median rotational bias found in pitcher, DKSup, and DKPro. In these tasks, OMC overestimated the BVR rotation values (Fig. 4a). The bias of the DKPro task was significantly greater than that for the flexion–extension task ($p < 0.05$) and the radial-ulnar deviation task ($p < 0.01$). The LOA range of rotation was different across tasks as well, with the median LOA range varying from 5.9° to 17.9°. The LOA range for the DKPro and pitcher tasks were significantly larger ($p < 0.05$) than the flexion–extension task (Fig. 4b).

There were no significant differences in the bias for translation ($p < 0.05$) across tasks. The median translation bias values ranged from −2.2 mm to 0.8 mm for the sample (Fig. 5a). The range of the LOA for translations for the circumduction task was significantly greater than the radial-ulnar deviation ($p < 0.05$) and pitcher pouring ($p < 0.05$) tasks (Fig. 5b).

All tasks except for the ϕ measurement in DKPro demonstrated that the differences between methods increased as the measurement average increased (supplemental materials for Bland-Altman plots). This trend was minimal for the flexion–extension task (0.3° difference per 10° change in average wrist rotation), and it was largest for the pitcher pouring (9° difference per 10° change in average wrist rotation) and DkSup (1.4° difference per 1° change in average rotation) tasks.

4. Discussion

We evaluated the agreement of OMC with BVR in measuring wrist motions during seven tasks to understand effects of soft tissue artifact on wrist kinematics. Task-based accuracy was observed.

OMC accuracy was previously quantified for *in-vitro* and *in-vivo* wrist postures (Hillstrom et al., 2014; Small et al., 1996). OMC can be considered a kinematic gold standard during *in-vitro* studies when marker sets contain at least 4 markers and are rigidly fixed to non-deformable objects (Challis, 1995; Söderkvist and Wedin, 1993). Hillstrom et al. evaluated OMC accuracy of *in-vitro* wrist postures in flexion–extension and radial-ulnar deviation using fluoroscopy as the reference. Hillstrom et al. summarized motion

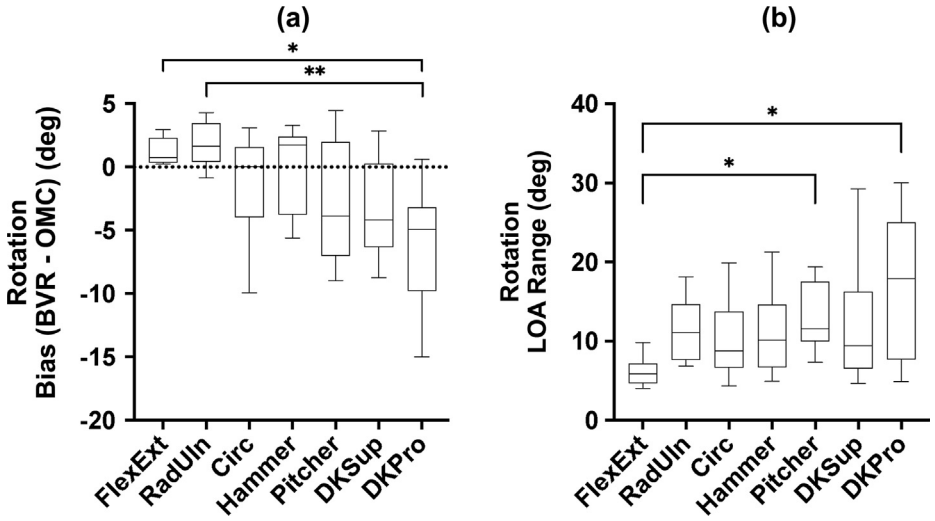

Fig. 4. Rotational Agreement Between Biplanar Videoradiography (BVR) and Optical Motion Capture (OMC). (a) Mean bias (BVR – OMC) across 9 subjects of the rotation about the screw axis (ϕ) by task, referencing BVR as the gold standard. (b) Range of the limit of agreement (LOA) across subjects of the rotation about the screw axis (ϕ) by task, referencing BVR as the gold standard.

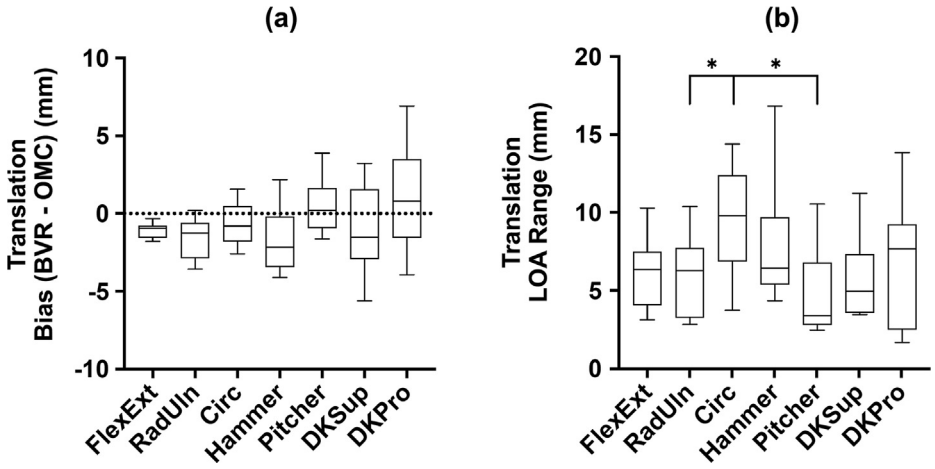

Fig. 5. Translational Agreement Between Biplanar Videoradiography (BVR) and Optical Motion Capture (OMC). (a) Mean bias (BVR – OMC) across 9 subjects of the translation along the screw axis by task, referencing BVR as the gold standard. (b) Range of the limit of agreement (LOA) across subjects of the translation along the screw axis by task, referencing BVR as the gold standard.

with euler angles and did not study translation. Small et al. quantified the error of OMC for *in-vivo* wrist kinematics comparing the surface markers to stereoradiography. Small et al. reported mean differences of ±2° and standard deviations <3° during flexion–extension and radial-ulnar deviation hand postures. Despite technology differences between stereoradiography and BVR, our median error in the radial-ulnar deviation and flexion–extension tasks aligned with the findings for mean difference. However, our experiment yielded larger variation, likely because we captured dynamic motion. Vardakastani et al. compared OMC measurements at the start and end points of flexion–extension, radial-ulnar deviation, and dart throwers motion. When comparing OMC to goniometry, Vardakastani et al. reported a mean difference of 25° (SD 16°). Despite technology differences, our study also showed large variation of *in-vivo* OMC accuracy depending on the task being performed (Vardakastani et al., 2018).

Previous studies have not compared OMC and BVR measurements during *in-vivo* wrist motion. Similar studies assessed the accuracy of OMC using BVR as the gold standard for ankle and knee (Kessler et al., 2019; Miranda et al., 2013). The ankle joint is comprised of several compact bones similar to the wrist but functions to accomplish much different tasks. OMC accuracy was evaluated using RMSE during walking and running and resulted in angular errors ranging from 1.1° to 8.3°. RMSE is not directly comparable to bias and LOA (Giavarina, 2015). Miranda et al. previously evaluated OMC accuracy compared to BVR during an *in-vivo* jump cup maneuver in the knee. The differences between OMC and BVR were assessed before and after ground contact. The study by Miranda et al. differed significantly from ours as the bones in the knee are larger than the bones in the wrist and our motions did not involve impact. A study was conducted on STA of 3 mm markers during various finger postures (Metcalf et al., 2020). The study reported an RMSE of 4° and did not assess dynamic motion. In larger joints like the knee and smaller joints in the fingers, both reported variation when studying joint kinematics with OMC surface markers.

Due to sample size and recruitment of only a single male subject, sex-based differences during *in-vivo* BVR and OMC kinematics could not be analyzed in this study. Skeletal wrist anatomy differs by sex, but to date only size has been documented as a difference so it is unlikely that sex alone would be a factor (Crisco et al.,

2005b; Schneider et al., 2015). More likely, BMI is a factor with larger skin deformation during certain tasks leading to larger STA, but our study was not designed or powered to examine BMI. Lastly, while the tasks we examined were dynamic, they did not involve impact, which has been shown to significantly increase STA (Miranda et al., 2013).

Declaration of Competing Interest

The authors declare that they have no known competing financial interests or personal relationships that could have appeared to influence the work reported in this paper.

Acknowledgements

We thank Erika Tavares for her help throughout biplanar videoradiography data acquisition, and Janine Molino for her help with the statistical analysis. This study was made possible with partial support from the National Institutes of Health P30-GM122732 (COBRE Bio-engineering Core) and a grant from the American Foundation for Surgery of the Hand (AFSH).

Appendix A. Supplementary material

Supplementary data to this article can be found online at https://doi.org/10.1016/j.jbiomech.2021.110362.

References

Aizawa, J., Masuda, T., Koyama, T., Nakamaru, K., Isozaki, K., Okawa, A., Morita, S., 2010. Three-dimensional motion of the upper extremity joints during various activities of daily living. J. Biomech. 43, 2915–2922. https://doi.org/10.1016/j.jbiomech.2010.07.006.

Akhbari, B., Moore, D.C., Laidlaw, D.H., Weiss, A.-P.-C., Akelman, E., Wolfe, S.W., Crisco, J.J., 2019a. Predicting carpal bone kinematics using an expanded digital database of wrist carpal bone anatomy and kinematics. J. Orthop. Res. https://doi.org/10.1002/jor.24435.

Akhbari, B., Morton, A., Moore, D., Weiss, A.-P.-C., Wolfe, S.W., Crisco, J.J., 2019b. Kinematic accuracy in tracking total wrist arthroplasty with biplane videoradiography using a CT-generated model. J. Biomech. Eng. https://doi.org/10.1115/1.4042769.

Akhbari, B., Morton, A.M., Moore, D.C., Weiss, A.-P.-C., Wolfe, S.W., Crisco, J.J., 2019c. Accuracy of biplane videoradiography for quantifying dynamic wrist kinematics. J. Biomech. 92, 120–125. https://doi.org/10.1016/j.jbiomech.2019.05.040.

Akhbari, B., Morton, A.M., Shah, K.N., Molino, J., Moore, D.C., Weiss, A.-P.-C., Wolfe, S.W., Crisco, J.J., 2020. Proximal-distal shift of the center of rotation in a total wrist arthroplasty is more than twice of the healthy wrist. J. Orthop. Res. 38, 1575–1586. https://doi.org/10.1002/jor.24717.

Bland, J.M., Altman, D.G., 1986. Statistical methods for assessing agreement between two methods of clinical measurement. Lancet 1, 307–310.

Brainerd, E.L., Baier, D.B., Gatesy, S.M., Hedrick, T.L., Metzger, K.A., Gilbert, S.L., Crisco, J.J., 2010. X-ray reconstruction of moving morphology (XROMM): precision, accuracy and applications in comparative biomechanics research. J. Exp. Zool A Ecol. Genet. Physiol. 313, 262–279. https://doi.org/10.1002/jez.589.

Challis, J.H., 1995. A procedure for determining rigid body transformation parameters. J. Biomech. 28, 733–737.

Crisco, J.J., Coburn, J.C., Moore, D.C., Akelman, E., Weiss, A.-P.-C., Wolfe, S.W., 2005a. In vivo radiocarpal kinematics and the dart thrower's motion. J. Bone Joint Surg. Am. 87, 2729–2740. https://doi.org/10.2106/JBJS.D.03058.

Crisco, J.J., Coburn, J.C., Moore, D.C., Upal, M.A., 2005b. Carpal bone size and scaling in men versus in women. J. Hand Surg. Am. 30, 35–42. https://doi.org/10.1016/j.jhsa.2004.08.012.

Cutti, A.G., Paolini, G., Troncossi, M., Cappello, A., Davalli, A., 2005. Soft tissue artefact assessment in humeral axial rotation. Gait Posture 21, 341–349.

D'Isidoro, F., Brockmann, C., Ferguson, S.J., 2020. Effects of the soft tissue artefact on the hip joint kinematics during unrestricted activities of daily living. J. Biomech. 104, 109717. https://doi.org/10.1016/j.jbiomech.2020.109717.

Garg, R., Kraszewski, A.P., Stoecklein, H.H., Syrkin, G., Hillstrom, H.J., Backus, S., Lenhoff, M.L., Wolff, A.L., Crisco, J.J., Wolfe, S.W., 2014. Wrist kinematic coupling and performance during functional tasks: effects of constrained motion. J. Hand Surgery 39, 634–642.e1. https://doi.org/10.1016/j.jhsa.2013.12.031.

Giavarina, D., 2015. Understanding Bland Altman analysis. Biochem. Med. (Zagreb) 25, 141–151 https://doi.org/10.11613/BM.2015.015.

Hillstrom, H.J., Garg, R., Kraszewski, A., Lenhoff, M., Carter, T., Backus, S.I., Wolff, A., Syrkin, G., Cheng, R., Wolfe, S.W., 2014. Development of an anatomical wrist joint coordinate system to quantify motion during functional tasks. J. Appl. Biomech. 30, 586–593. https://doi.org/10.1123/jab.2011-0094.

Kessler, S.E., Rainbow, M.J., Lichtwark, G.A., Cresswell, A.G., D'Andrea, S.E., Konow, N., Kelly, L.A., 2019. A direct comparison of biplanar videoradiography and optical motion capture for foot and ankle kinematics. Front. Bioeng. Biotechnol. 7, 199. https://doi.org/10.3389/fbioe.2019.00199.

Knörlein, B.J., Baier, D.B., Gatesy, S.M., Laurence-Chasen, J.D., Brainerd, E.L., 2016. Validation of XMALab software for marker-based XROMM. J. Exp. Biol. 219, 3701–3711. https://doi.org/10.1242/jeb.145383.

Metcalf, C.D., Phillips, C., Forrester, A., Glodowski, J., Simpson, K., Everitt, C., Darekar, A., King, L., Warwick, D., Dickinson, A.S., 2020. Quantifying soft tissue artefacts and imaging variability in motion capture of the fingers. Ann. Biomed. Eng. 48, 1551–1561. https://doi.org/10.1007/s10439-020-02476-2.

Miranda, D.L., Rainbow, M.J., Crisco, J.J., Fleming, B.C., 2013. Kinematic differences between optical motion capture and biplanar videoradiography during a jump-cut maneuver. J. Biomech. 46, 567–573. https://doi.org/10.1016/j.jbiomech.2012.09.023.

Miranda, D.L., Schwartz, J.B., Loomis, A.C., Brainerd, E.L., Fleming, B.C., Crisco, J.J., 2011. Static and dynamic error of a biplanar videoradiography system using marker-based and markerless tracking techniques. J. Biomech. Eng. 133, 121002. https://doi.org/10.1115/1.4005471.

Panjabi, M.M., Krag, M.H., Goel, V.K., 1981. A technique for measurement and description of three-dimensional six degree-of-freedom motion of a body joint with an application to the human spine. J. Biomech. 14, 447–460.

Schmidt, R., Disselhorst-Klug, C., Silny, J., Rau, G., 1999. A marker-based measurement procedure for unconstrained wrist and elbow motions. J. Biomech. 32, 615–621.

Schneider, M.T.Y., Zhang, J., Crisco, J.J., Weiss, A.P.C., Ladd, A.L., Nielsen, P., Besier, T., 2015. Men and women have similarly shaped carpometacarpal joint bones. J. Biomech. 48, 3420–3426. https://doi.org/10.1016/j.jbiomech.2015.05.031.

Small, C.F., Bryant, J.T., Dwosh, I.L., Griffiths, P.M., Pichora, D.R., Zee, B., 1996. Validation of a 3D optoelectronic motion analysis system for the wrist joint. Clin. Biomech. (Bristol, Avon) 11, 481–483.

Söderkvist, I., Wedin, P.-Å., 1993. Determining the movements of the skeleton using well-configured markers. J. Biomech. 26, 1473–1477. https://doi.org/10.1016/0021-9290(93)90098-Y.

Tashman, S., Anderst, W., 2003. In-vivo measurement of dynamic joint motion using high speed biplane radiography and CT: application to canine ACL deficiency. J. Biomech. Eng. 125, 238–245.

Vardakastani, V., Bell, H., Mee, S., Brigstocke, G., Kedgley, A.E., 2018. Clinical measurement of the dart throwing motion of the wrist: variability, accuracy and correction. J. Hand Surg. Eur. 43, 723–731. https://doi.org/10.1177/1753193418773329.

Wolfe, S.W., Crisco, J.J., Orr, C.M., Marzke, M.W., 2006. The dart-throwing motion of the wrist: is it unique to humans?. J. Hand Surg. Am. 31, 1429–1437. https://doi.org/10.1016/j.jhsa.2006.08.010.